Sains Malaysiana 51(5)(2022): 1511-1524
http://doi.org/10.17576/jsm-2022-5105-20

Volume Shrinkage during Carbothermic Reduction of Low-Grade Iron Ore Containing Goethite and Coal Composite

(Pengecutan Isi Padu semasa Pengurangan Karbotermik Komposit Bijih Besi Gred Rendah yang Mengandungi Goetit dan Arang)

AGUNG SETIAWAN[1], INA ERMAWATI[1], FARRAS ANGGRAINI[1], FAIZINAL ABIDIN[2], ABDUL HAPID[3], ADJI KAWIGRAHA[3], SRI HARJANTO[1,*] & M. AKBAR RHAMDHANI[4]

[1]*Department of Metallurgical and Materials Engineering, Faculty of Engineering, Universitas Indonesia, 16424 Kampus Baru UI Depok, West Java, Indonesia*
[2]*Directorate of Utilization of Research and Innovation by Government, Society, and Micro, Small, and Medium Enterprises- National Research and Innovation Agency (BRIN), Jakarta 10340, Indonesia*
[3]*Research Center for Mining Technology, National Research and Innovation Agency (BRIN), Building 820, Puspitek, Banten 15314, Indonesia*
[4]*Fluid and Process Dynamics (FPD) Research Group, Department of Mechanical and Product Design Engineering, Swinburne University of Technology, Melbourne, VIC 3122, Australia*

Received: 7 June 2021/Accepted: 20 October 2021

ABSTRACT

The volume shrinkage and reduction behavior of low-grade iron ore goethite during the solid-state carbothermic process was studied and compared to synthetic goethite. The carbothermic reduction process using low-grade coal as a reducing agent was carried out in the temperature range 1000-1200 °C up to 60 min of reaction time. The results demonstrated that the volume shrinkage, reduction degree, and metallization degree of reduced samples increase with increasing temperature and reaction time. Compared to the reduced samples using synthetic goethite, the volume shrinkage, reduction degree, and metallization degree of the reduced samples using iron ore are lower due to the presence of impurities in Sebuku iron ore concentrates, which include Mg, Mn, Al, and Si. The highest volume shrinkage observed at 1200 °C for 60 min reaction time for the reduced samples using iron ore and synthetic goethite was 63.57±0.57 and 76.51±1.53%, respectively. The observed phases at this point were metallic iron (Fe_m) and spinel $(Fe,Mg)Al_2O_4$. The volume shrinkage of the reduced samples was caused primarily by the weight loss due to carbon, oxygen, and combined water evaporation, as well as the sintering of gangue oxides and metallic iron particles, and partial melting of these phases.

Keywords: Direct reduction; goethite; low-grade iron ore; rotary hearth furnace; volume shrinkage

ABSTRAK

Pengecutan isi padu dan tingkah laku pengurangan bijih besi kelas rendah yang mengandungi goetit semasa proses karbotermik keadaan pepejal dikaji berbanding dengan goetit sintetik. Proses pengurangan karbotermik menggunakan arang batu rendah sebagai agen pengurangan dilakukan dalam julat suhu 1000-1200 °C hingga 60 min masa reaksi. Hasil kajian menunjukkan bahawa pengecutan isi padu, tahap pengurangan dan tahap pengukuran sampel yang dikurangkan meningkat dengan peningkatan suhu dan tindak balas masa. Berbanding dengan sampel yang dikurangkan menggunakan goetit sintetik, pengecutan isi padu, tahap pengurangan dan tahap metalisasi sampel yang dikurangkan menggunakan bijih besi lebih rendah kerana beberapa kekotoran dalam pekatan bijih besi Sebuku, termasuk Mg, Al dan Si. Nilai pengecutan isi padu tertinggi yang dijumpai pada suhu 1200 °C selama 60 min masa reaksi bagi sampel yang dikurangkan menggunakan bijih besi dan goetit sintetik masing-masing adalah 63.57±0.57 dan 76.51±1.53%. Fasa yang diamati pada ketika ini adalah besi logam (Fe_m) dan spinel $(Fe,Mg)Al_2O_4$. Pengecutan jumlah sampel yang dikurangkan disebabkan terutamanya oleh penurunan berat badan karbon, oksigen dan air gabungan dan pertumbuhan sintering oksida gangue dan zarah besi logam dan pencairan sebahagian fasa gangue.

Kata kunci: Bijih besi bermutu rendah; goetit; pengecutan isi padu; pengurangan langsung; relau perapian putar

INTRODUCTION

Steel production in the last two years reached more than 1.7 billion tons, which indicates that iron and steel consumption continues to grow as the global economy progresses, particularly in developing countries (World Steel Association 2020). High-grade iron ore is the most commonly used iron mineral for producing high-grade iron and steel. However, the main challenge in the current iron and steel production is the depletion of high-grade iron reserves (Yellishetty et al. 2010). Therefore, developing a new process that can utilize low-grade iron ore to substitute high-grade iron ore is essential.

Recently, some researchers have developed the upgrading process of low-grade iron ore containing goethite. Low-grade iron ore such as goethite, α-FeOOH, contains high concentration water and gangue minerals (Al, Si, Mg, and Mn) which needs further attention to before it can be used as source for iron and steel production. Goethite has a layered structure which is a combination of hydrogen bonds chained to OH group which can liberate through endothermic reaction at 200-300 °C through water (H_2O) and vapor (H_2O) formation (Miura et al. 2011).

A beneficiation of Indian goethite-rich iron ore via reduction roasting followed by low-intensity magnetic separation was reported by Ravisankar et al. (2019). They reported that after the magnetic separation and reduction process at 800 °C with 10% coal for 30 min, 90.44% of the 66.58% Fe existed in the ore was recovered. Abd Rashid et al. (2014) completely reduced Malaysian low-grade iron ore to magnetite, wustite, and partially metallic iron at 900 °C using biomass. The process was controlled by a chemical reaction with the activation energy of 115 kJ.mol^{-1}. Setiawan et al. (2019) used biomass as a reducing agent and successfully produced a pig iron nugget from Lampung low-grade iron ore, with a reduction degree of 98.5% and metallization degree of 99.2%.

A reduction process of low-grade iron and complex iron ore based on the rotary hearth furnace (RHF) technology has drawn the attention of researchers recently. This technology is using a circular-shaped refractory reactor, utilizing waste oxides, fine particulate material, and mills to generate direct-reduced iron (DRI) which resulted from the reduction of mixed oxides with carbon reductant (such as coal) in composite pellets (Halder & Fruehan 2008a). However, due to the impediment of heat transfer to the lower layers of the bed, one of the shortcomings of the RHF ironmaking process is the inability to use multiple composite pellets.

It has been reported that pellets shrinkage strongly impacts the kinetics by improving the external heat transfer to the lower layers (Halder & Fruehan 2008b). Halder and Fruehan (2008b) reported that the heat transfer to the second level increases by almost 6 times if the pellets at the top layer are shrinking by 30%. The maximum volume shrinkage of a ludwigite-anthracite composite pellet was reported to be 55.55% at 1300 °C after 30 min of reaction. The activation energy of solid-state reduction of pellet samples at 1150 to 1250 °C was reported to be 276 kJ/mol (Wang et al. 2015).

Wang et al. (2018) investigated the volume shrinkage kinetics of magnetite-anthracite composite pellet during carbothermic reduction at 1050 to 1200 °C. They found that the shrinkage activation energy varies depending on the reaction time. The shrinkage activation energy was reported to be 51.31 J/mol during the first 20 min and decreased to 19.7 J/mol after that. The change in the reduction rate-controlling step and the automatic sintering and reconstruction of metallic iron particles and gangue oxides in the later reduction stage were suggested to be the primary cause of these time-dependent phenomena (Wang et al. 2018).

Nevertheless, the volume shrinkage behavior of iron containing goethite/low-grade coal composite pellet during the carbothermic reduction process has not been extensively discussed in the published literature. There are limited studies related to swelling in low-grade iron ore and its association with the growth of iron whiskers (Ogbezode et al. 2021; Prusti et al. 2021). In the current work, the volume shrinkage and general reduction behavior of goethite iron ore were studied and compared to synthetic goethite during a reduction using low-grade coal as a reducing agent to provide useful information for the optimization of low-grade iron ore direct reduction technologies.

MATERIALS AND METHODS

MATERIALS

The raw materials used in this research were synthetic and natural goethite ores. The goethite ore (low-grade iron ore) was obtained from Sebuku Island, South Kalimantan (Borneo) Province, Indonesia. The bulk chemical analysis of Sebuku ore, determined using x-ray fluorescence (XRF), is shown in Table 1. It can be seen that Sebuku ore has a high content of iron, i.e., 45.50 wt.%. The major impurities in the ore sample include Al (6.19 wt.%), Si (2.10 wt.%), and Mn (1.11 wt.%). In addition, the ore sample also contains a small number of other impurities (e.g. Ni, S, Mg, Ti, and Ca). The phases present in the Sebuku ore, examined by x-ray diffraction (XRD), are shown in Figure 1, which indicate that the main phases in the ore are goethite, hematite, and magnetite.

TABLE 1. Chemical compositions of materials used in the experiment, in wt.%

Content	Sebuku ore	Synthetic goethite
Fe	45.50	63.70
Al	6.19	-
Si	2.10	0.136
Mn	1.11	0.322
Ni	0.613	49.10*
S	0.576	0.716
Mg	0.566	-
Ti	0.19	-
Ca	0.068	0.270
P	-	0.0086
K	-	0.0121
Na	-	0.0116
Cr	-	114.00*
As	-	15.10*
Cl	-	30.10*
Cu	-	12.60*
Co	-	11.00*
Ba	-	60.60*
V	-	5.26*
Za	-	44.60*

* in ppm

Synthetic goethite from Sigma-Aldrich was also used as a sample control in this study. The chemical analysis and phase compositions of the synthetic goethite were determined by XRF and XRD, respectively. The XRF result (Table 1) indicated that the synthetic goethite contains 63.70 wt.% of Fe, and XRD analysis (Figure 1) confirmed that the main phase is FeOOH.

Sub-bituminous coal was used as a reducing agent. The proximate and ultimate analysis of coal were measured according to the ASTM D.3172 (for fixed carbon), ASTM D.3175 (for the volatile matter), ASTM D.3174 (for ash), ASTM D.3173 (for moisture in air-dried), ASTM D.4239 (for total Sulphur), ASTM D.5373

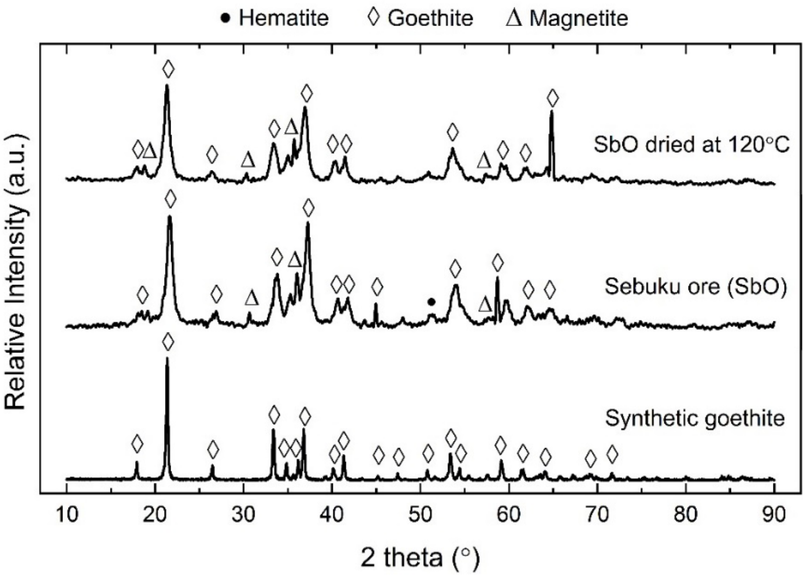

FIGURE 1. XRD analysis of synthetic goethite and Sebuku ore as received and after dried at 120 °C for 2 h

(for carbon, hydrogen, and nitrogen), ASTM D.3176 (for oxygen). As shown in Table 2, the coal is low in fixed carbon (38.52 wt.%) and high in the volatile matter (31.18 wt.%).

Bentonite and calcium carbonate were used as a binder and a flux, respectively. The major chemical compositions of bentonite examined by XRF were Si, Al, Fe, and Mg, while the XRD results confirmed the major phase $CaCO_3$ with 97.8% in concentration.

TABLE 2. Analysis of proximate and ultimate of sub-bituminous coal, in wt.%

Analysis	Parameters	Content
Proximate	Fixed carbon	38.52
	Volatile matter	31.18
	Moisture	5.54
	Ash	24.76
Ultimate	Carbon	51.85
	Hydrogen	4.51
	Nitrogen	1.45
	Total Sulphur	1.63
	Oxygen	15.80

PREPARATION OF COMPOSITE PELLETS

Sebuku ore was pulverized to homogenize the particle size and then dried at 120 °C for 2 h. The particle size of the Sebuku ore was measured using Cilas 1190 laser particle size analyzer (PSA). Figure 2 shows that the mean particle size of the iron ore was 12.75 µm with D_{80} 22.74 µm.

Each raw material (dried Sebuku ore and synthetic goethite) was mixed homogeneously with coal, bentonite, and calcium carbonate, with the respective compositions as listed in Table 3.

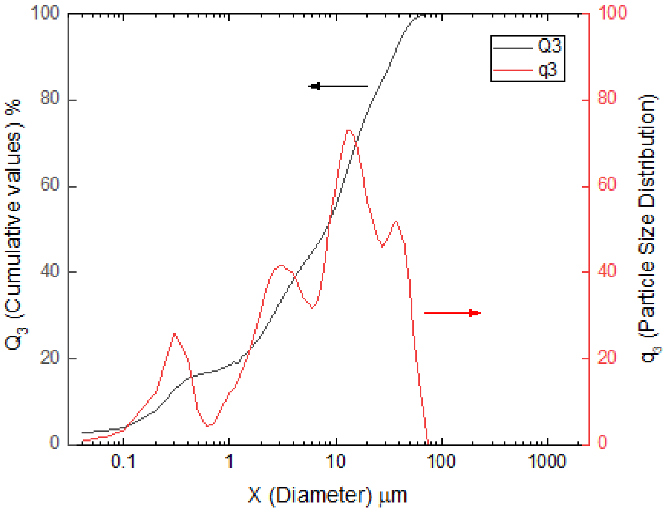

FIGURE 2. The result of PSA test on Sebuku ore

TABLE 3. Compositions of the material mixture, in wt.%

Samples	Iron ore*	Coal	Bentonite	Calcium carbonate
SbO-1	69	24	2	5
SbO-2	77	16	2	5
SyG-1	69	24	2	5
SyG-2	77	16	2	5

* SbO: Sebuku ore; SyG: synthetic goethite

The mixture of fifteen-gram was shaped into pellets (diameter of ~1.25 cm) using a pelletizing machine by spraying water, as shown in Figure 3.

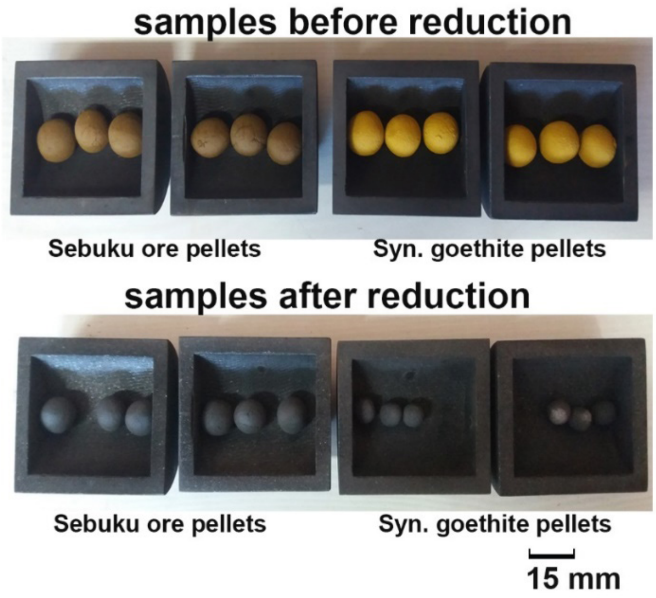

FIGURE 3. The pelleted samples before and after the carbothermic reduction process

CARBOTHERMIC REDUCTION

The carbothermic reduction process was carried out in a horizontal tube furnace with U-type $MoSi_2$ heating elements and type-B thermocouple. Six pelleted samples from each ore were placed in graphite crucible boats and put into the hot zone of the tube furnace, as shown in Figure 4. Nitrogen gas was flown into the furnace chamber with flow rate of 0.8 L/min to maintain an inert atmosphere. The samples were heated at 1000 to 1200 °C with reaction time of 30 to 60 min, and the heating rate of 10 °C/min. After the reduction experiment, the samples were cooled to room temperature inside the closed tube furnace.

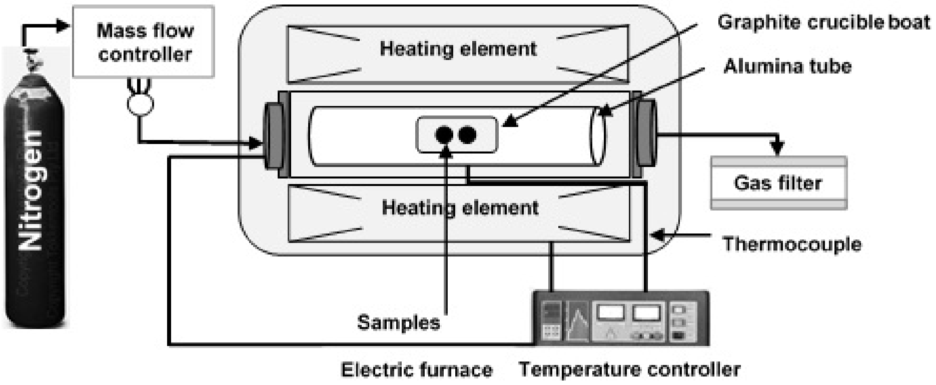

FIGURE 4. A schematic diagram of carbothermic reduction process equipment setup

ANALYSIS AND CHARACTERIZATION

For XRD analysis, the reduced samples (in the form of powder) were examined using x-ray diffraction, Rigaku MiniFlex PDXL, with a Cu Kα source (λ=1.54178 Å) to identify phase compositions. The XRD machine was operated at 15 mA and 30 kV with scanning from 10° to 90° (2θ) with a scan speed 4° per min. Phase identification and quantitative phase analysis (QPA) were carried out using Match! Software.

The reduced samples' surface morphology and elemental analysis were investigated using field-emission scanning electron microscopy, FE-SEM (JEOL JSM-7500FA), and Energy Dispersive X-ray spectroscopy (EDX) with an accelerating voltage of 20 kV. Before characterization, the reduced samples were mounted in epoxy resin and polished with silicon carbide paper up to 1200-grit followed by alpha alumina powder paste (1 µm). After ultrasonic cleaning, the samples were coated with Au-Pd by sputtering in a vacuum.

A NETZSCH STA 449 F1 Jupiter STA (Simultaneous Thermal Analysis) unit was utilized to analyze the thermal characteristics. Before running the test, the sensor was calibrated using certified reference materials to correct sensitivity coefficients and temperature calibration. The powder sample of 5±0.5 mg was loaded into an alumina pan and heated from 30 to 1200 °C with a heating rate of 10 °C/min.

Volume shrinkage (Sh) of the reduced samples was calculated using Equation (1) (Halder & Fruehan 2008b). The diameter of the six pellets from each ore sample were measured before and after the reduction process.

$$\mathrm{Sh} = \frac{(\mathrm{Di}-\mathrm{Dr})}{\mathrm{Di}} \times 100\% \qquad (1)$$

where Di and Dr are the initial diameter of the pellet sample and the final diameter of the reduced samples, respectively.

The reduction degree, RD, was calculated based on the percentage of oxygen mass in the sample calculated using QPA. The calculation was made by considering that iron ore contains only the goethite phase and using the following Equation (2):

$$\mathrm{RD} = \frac{(\mathrm{mO_i}-\mathrm{mO_f})}{\mathrm{mO_i}} \times 100\% \qquad (2)$$

where mO_i and mO_f are the initial mass of oxygen and the final mass of oxygen in the sample, respectively.

The metallization degree (MD) of the reduced sample was determined using the titration method (iron chloride method) following Equation (3).

$$\mathrm{MD} = \frac{MFe}{TFe} \times 100\% \tag{3}$$

where TFe and MFe are the total iron and the mass fraction of metallic iron in the sample, respectively.

RESULTS AND DISCUSSION

THERMAL AND REDUCTION BEHAVIOR OF THE SAMPLES

Thermal properties of the samples were analyzed using thermogravimetric analysis (TGA), derivative thermogravimetry (DTG) as well differential thermal analysis (DTA). The analyses were carried out in an inert atmosphere from ambient to 1200 °C, and the results are shown in Figure 5. The thermogravimetric curves from the samples show six weight loss steps, and these are listed in more detailed in Table 4. The total weight losses of the samples using Sebuku ore (SbO-1 and SbO-2) and synthetic goethite (SyG-1 and SyG-2) are 39.28%, 34.07%, 43.52%, and 35.71%, respectively.

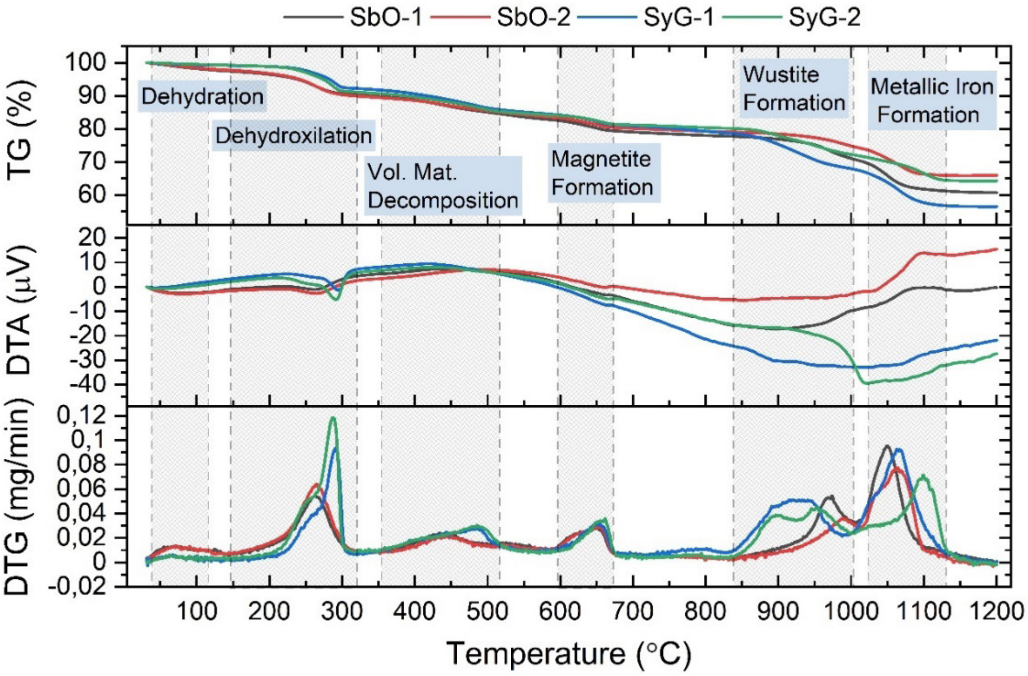

FIGURE 5. The thermal properties result of samples Sebuku ore (SbO-1 and SbO-2) and synthetic goethite (SyG-1 and SyG-2)

The initial weight loss in all samples occurred below 120 °C which likely to be from water dehydration, i.e. removal of absorbed water from the samples. Ghose et al. (2010) suggested two types of adsorbed water and terminal hydroxyls on the goethite surface, with an interface stoichiometry of ((H_2O)–(H_2O)–OH_2–OH–Fe–O–O–Fe–R). The temperature range of water dehydration observed in this study is similar to that reported by Ponomar (2018) for natural and synthetic goethite heated from ambient to 120 °C. In addition, the weight loss from Sebuku ore samples (SbO-1 and SbO-2) was found to be slightly bigger compared to that from synthetic goethite samples (SyG-1 and SyG-2). It is suggested that this may be due to the slightly different mineralogy of goethite ore.

TABLE 4. Weight loss of samples using Sebuku ore (SbO) and synthetic goethite (SyG)

Reaction	Weight loss of samples (%)			
	SbO-1	SbO-2	SyG-1	SyG-2
Dehydration	2.12	1.88	0.72	0.58
Dehydroxylation	7.63	8.19	7.04	8.27
Volatile matter decomposition	5.77	4.90	6.49	5.92
Fe_3O_4 formation	5.07	4.62	4.50	3.80
FeO formation	8.31	5.57	13.28	9.15
Fe_m formation	10.38	8.91	11.49	7.99

The second weight loss occurred between 150 and 320 °C according to the DTG curves. The loss is associated with the dehydroxylation process occurring due to the transformation of goethite (FeOOH) to hematite (Fe_2O_3). Similar observations were reported by other researchers using synthetic goethite samples (Ford & Bertsch 1999), pure goethite (Weissenborn et al. 1994), and goethite ore-biomass samples (Wang et al. 2015).

The peak temperature of dehydroxylation was observed at 264 °C for Sebuku ore samples (SbO-1 and SbO-2). However, a double peak of goethite-hematite transformation was observed for synthetic goethite samples (SyG-1 and SyG-2). In addition, the endothermic peak of synthetic goethite samples (SyG-1 and SyG-2) was found to be slightly higher than that from Sebuku ore samples (SbO-1 and SbO-2). Schwertmann (1984) reported that the double peaks at 200 to 300 °C represent a high crystallinity of goethite. A low crystalline goethite can complete a transformation to hematite before the unit cell size changes. On the other hand, high crystalline goethite would exhibit a change in unit cell size which occurs at a higher temperature (Schwertmann 1984). Similar results were also reported by other researchers where two peaks of dehydroxylation observed between 172 and 310 °C (Liu et al. 2013) and between 270 and 401 °C (McCann et al. 2004). Thus, our results are in good agreement with these previous reports.

The following weight loss occurs between 350 and 520 °C. This loss is caused by the decomposition of volatile matter of sub-bituminous coal. Sarkar et al. (2016) reported a similar result of a significant weight loss observed over 400 °C which due to the release of the majority of the volatile matters in low-rank coal. Ravisankar et al. (2019) also reported a weight loss of carbon at 500 °C when using non-coking coal as a reducing agent on beneficiation of goethite-rich iron ore.

The fourth weight loss occurred between 600 and 680 °C. This loss is caused by the magnetite (Fe_3O_4) formation. The formation of magnetite (Fe_3O_4), by a diffusion process of reducing gas (CO), was taken place on the hematite (Fe_2O_3) particle surface (Yu & Qi 2011). Valix and Cheung (2002) reported that at 600 and 700 °C, using a reducing potential of 1:1 CO:CO_2, goethite (α-FeOOH) phase completely transforms into magnetite (Fe_3O_4). Jang et al. (2014) reported the transformation of goethite (FeOOH) to magnetite (Fe_3O_4) via a reduction process in a CO/CO_2 gas environment at 650 and 700 °C. Another researcher also reported a complete transformation to magnetite (Fe_3O_4) at 650 °C during reductions of synthetic and natural brown goethite with starch as a reductant (Ponomar 2018).

The fifth weight loss occurred between 840 and 1000 °C. The loss is associated with magnetite (Fe_3O_4) transformation to wustite (FeO) through direct/indirect reduction. A similar transformation to wustite (FeO) was reported during the reaction of ludwigite iron concentrate and anthracite at 1000 °C for 30 min (Wang et al. 2015). Furthermore, the final weight loss between 1020 and 1140 °C is associated with wustite (FeO) reduction to metallic iron (Fe_m).

The reduction and metallization degree of the reduced Sebuku (SbO-1 and SbO-2) and synthetic goethite (SyG-1 and SyG-2) samples at different temperatures and reaction times are shown in Figure 6(a) and 6(b), respectively. Generally, the figure shows that the reduction and the metallization degree increase

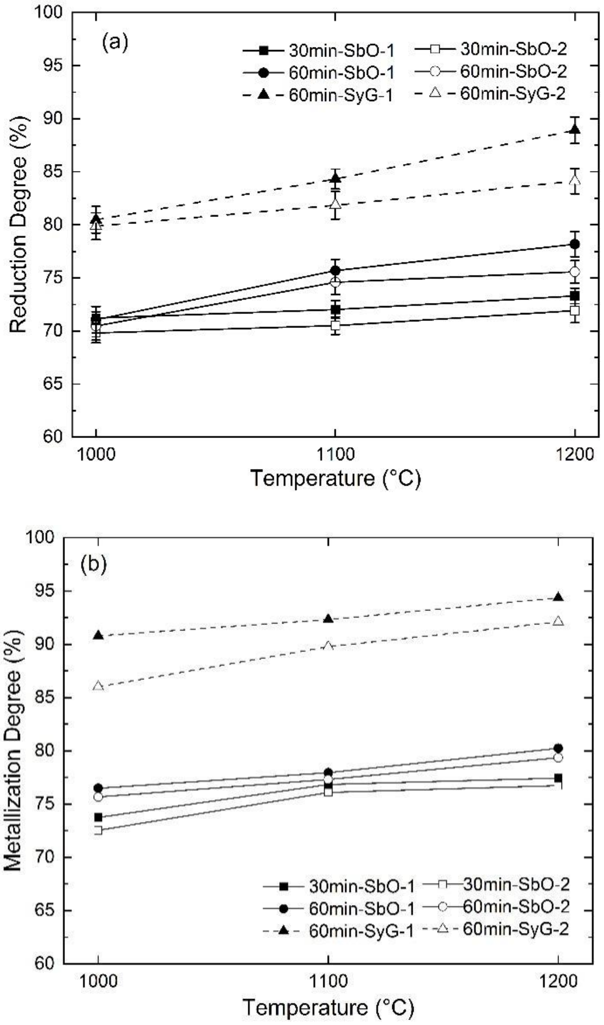

FIGURE 6. (a) Reduction degree and (b) Metallization degree of reduced samples using Sebuku ore (SbO-1 and SbO-2) and synthetic goethite (SyG-1 and SyG-2) at different temperature and reaction time

with increasing reduction temperature and time. When reductant (carbon) content is increased, e.g. in SbO-1 and SyG-1 samples compared to SbO-2 and SyG-2 samples, the reduction and the metallization degree are also increased. Increasing the carbon content in the pellet, the samples will also increase the production of CO-reducing gas, thus also increasing the CO/CO_2 ratio (Boudouard reaction) and speeding up the reduction process. The highest reduction and metallization degree from the Sebuku SbO-1 sample are 78.18±1.18 and 80.24%, respectively, at 1200 °C for 60 min. The SyG-1 sample exhibited higher reduction and metallization degrees compared to the Sebuku iron ore, i.e., 88.91±1.25 and 94.35%, respectively.

Furthermore, the reduction and metallization degree of the Sebuku iron ore are lower due to the presence of several impurities, including magnesium, manganese, aluminum, and silica. It is known that magnesium and manganese oxides act as a barrier to prevent complete Fe^{2+} reduction as well as carbon monoxide diffusion (Merk & Pickles 1988).

VOLUME SHRINKAGE OF PELLET SAMPLES DURING THE REDUCTION PROCESS

The volume shrinkage of pellet samples during the carbothermic reduction process, generally, is caused by the loss of oxygen, combined water, and carbon from the system; as well as the formation of metallic iron particles and liquid slag phase within the pellet samples (Halder & Fruehan 2008b). The volume shrinkage of the Sebuku (SbO-1 and SbO-2) and synthetic goethite (SyG-1 and SyG-2) ores at different temperatures and reaction times are shown in Figure 7. It can be observed that the volume shrinkage is highly dependent on the reduction temperature and reaction time. The volume shrinkage is closely related to the thermal history, reduction degree, and metallization degree.

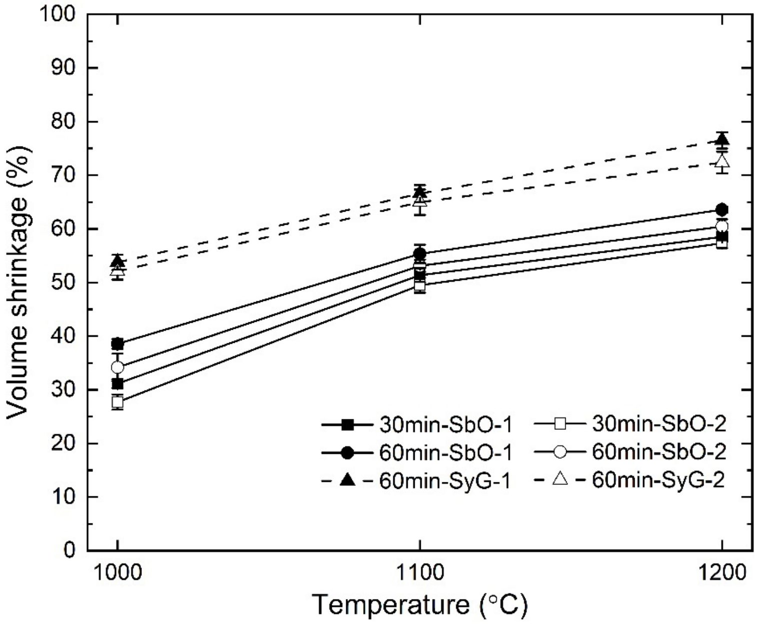

FIGURE 7. Volume shrinkage of reduced samples using Sebuku ores (SbO-1 and SbO-2) and synthetic goethite (SyG-1 and SyG-2) at different temperatures and reaction times

The shrinkages at 1000 °C after 30 min reaction for Sebuku ore samples (SbO-1 and SbO-2) were quite small, i.e. 31.15±0.79 and 27.71±1.40%, respectively. These phenomena were consistent with the fact that both of these samples have a low degree of reduction and metallization. Figure 8 shows the SEM images of these samples. It can be observed that there is a small amount of unreacted coal in the sample, indicating the early stage of reaction. Higher temperature and longer reaction time are expected to increase the extent of reaction and overall reduction rate.

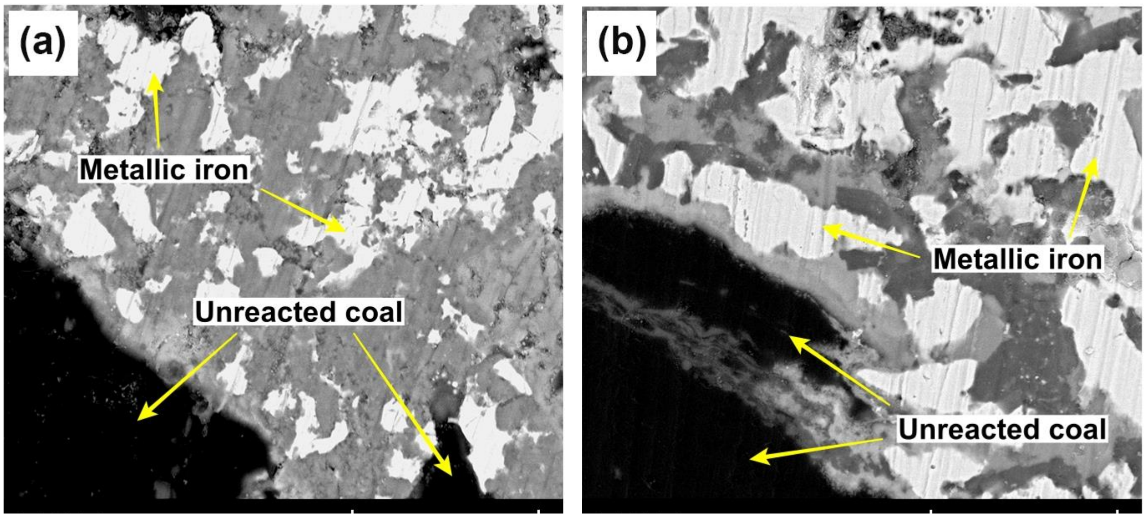

FIGURE 8. SEM back-scattered electron images of reduced samples for (a) Sebuku ore 2 (SbO-2) and (b) Sebuku ore 1 (SbO-1) at 1000 °C after 30 min of reaction

As the reaction time was increased from 30 to 60 min at 1000 °C, the shrinkage was observed to increase to 34.19±2.56% for SbO-2, 38.55±0.90% for SbO-1, 52.09±1.55% for SyG-2, and 53.77±1.4% for SyG-1. These samples were also analyzed using XRD and the results are presented in Figure 9. It can be seen that the major phases observed include metallic iron (Fe_m) and spinel $(Fe,Mg)Al_2O_4$. Wustite (FeO) phase, however, was detected in the synthetic goethite 2 (SyG-2) and Sebuku iron ore 2 (SbO-2) samples. This may be due to the low content of the reductant; hence it was not enough to reduce the goethite (FeOOH) phase during the heating process.

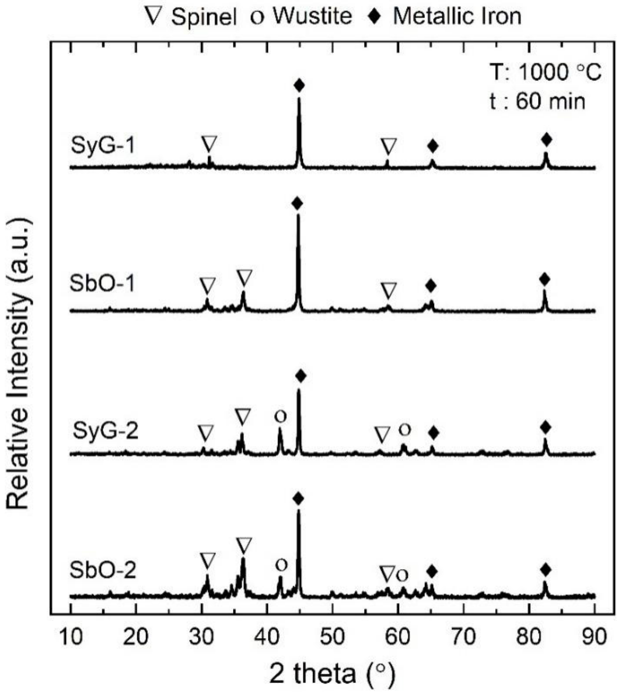

FIGURE 9. XRD analysis results of Sebuku ore (SbO-1 and SbO-2) and synthetic goethite (SyG-1 and SyG-2) reduced at 1000 °C for 60 min

Selected reduced samples were characterized using SEM back-scattered electron imaging to identify and confirm the formed phases. Figure 10 shows the BSE images of Sebuku iron ore 2 (SbO-2) and synthetic goethite 2 (SyG-2) samples reduced at 1000 °C for 60 min. The red dots are the area where EDX point analyses were carried out.

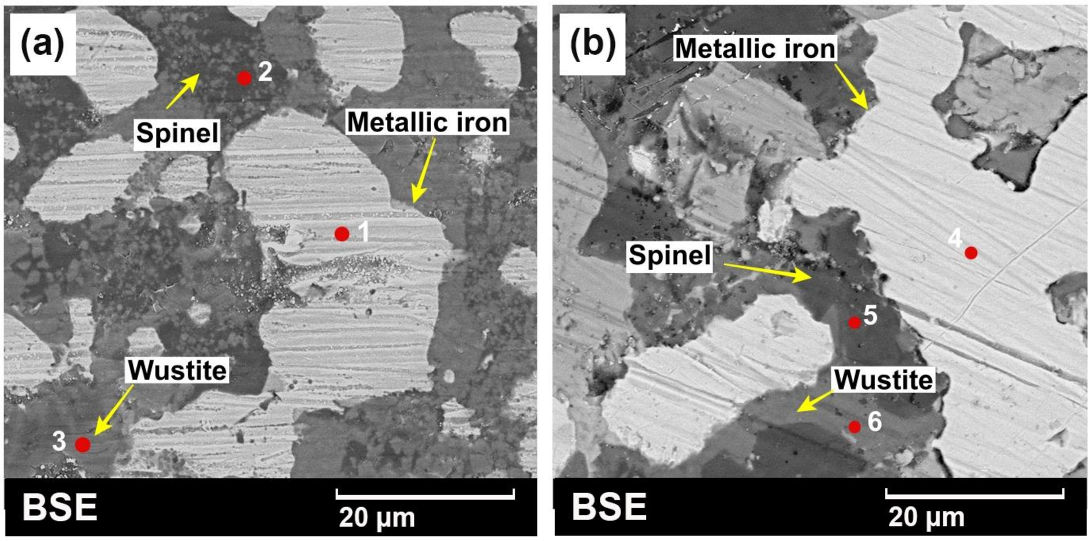

FIGURE 10. Back-scattered electron images of (a) Sebuku ore 2 (SbO-2) and (b) synthetic goethite 2 (SyG-2) samples reduced at 1000 °C for 60 min. Red points refer to EDX analysis results listed in Table 5

It can be seen from Figure 10 that the SEM images confirmed the XRD analysis results on the major phases present after reduction, i.e. metallic iron (Fe_m), spinel $(Fe,Mg)Al_2O_4$, and wustite (FeO). Furthermore, the morphology of metallic iron (Fe_m) in the SyG-2 sample (Figure 10b) appeared to be denser forming large Fe_m island network compared to SbO-2 sample (Figure 10a). This provides further evidence that the reduction and metallization degree in the synthetic goethite were higher compared to that in the Sebuku iron ore. In addition, semi-quantitative EDX analysis was conducted on the metallic iron (Fe_m), wustite (FeO), and spinel $(Fe,Mg)Al_2O_4$ phases, and the results are listed in Table 5. The Fe concentrations of the metallic iron (Fe_m) in the Sebuku ore-2 (SbO-2) and synthetic goethite-2 samples (SyG-2) were found to be quite higher, i.e. 93.45 and 94.77%, respectively. The minor impurities in these metallic irons (Fe_m) include Al, Si, Mg, Mn, and C.

TABLE 5. EDX results of areas/points for the metallic iron, wustite, and spinel phases in the area indicated in Figure 10. Data are semi-quantitative and have been normalized to 100 wt.%

Element	Point (wt.%)					
	1 Fe_m	2 Spinel	3 Wustite	4 Fe_m	5 Spinel	6 Wustite
Fe	93.45	16.71	68.46	94.77	18.58	69.34
O	1.97	35.28	27.32	2.38	38.18	27.00
Al	0.43	28.26	0.67	n.d.	24.38	0.39
Si	0.68	3.43	0.34	0.36	0.49	0.31
Mn	0.54	1.29	0.53	0.43	1.85	0.53
Mg	0.78	15.03	0.38	n.d.	16.52	0.19
C	2.15	n.d.	2.3	2.06	n.d.	2.24

As shown in Figure 7, increasing the temperature up to 1100 °C resulted in the increase of the volume shrinkage to 53.10±1.15% for SbO-2, 55.35±1.69% for SbO-1, 64.94±2.38% for SyG-2, and 66.58±1.57% for SyG-1. Because of a faster reaction rate at higher temperatures, the volume shrinkage also increases faster, accompanied by rapid rate of carbon and oxygen loss from the pellet, as well as a faster rate of sintering of the metallic iron particle and gangue oxides (Wang et al. 2015). Figure 11(a) shows the XRD results of samples reduced at 1100 °C for 60 min. The wustite (FeO) phase disappeared (as shown in Figure 9) at 1100 °C. Furthermore, the intensity of the spinel $(Fe,Mg)Al_2O_4$ peaks are quite weak and almost disappear for SyG-1 and SbO-1 samples.

The highest volume shrinkages were observed at 1200 °C, i.e. 60.44±1.35% for SbO-2, 63.57±0.57% for SbO-1, 72.35±2.01% for SyG-2, and 76.51±1.53% for SyG-1 samples. These results are much higher compared to the previous results (about 45%) when using ludwigite/coal composite and magnetite/carbon composite reduced at 1200 °C for 30 min (Wang et al. 2018, 2015). It can be seen from the XRD results (Figure 11b) that the intensity of the spinel $(Fe,Mg)Al_2O_4$ peaks nearly disappeared for the SyG-1, SyG-2, and SbO-1 samples.

Considering the results from the thermal, XRD, SEM, and EDX analyses, there are a number of possible reactions and phase transformations occurring when the samples were heated from ambient temperature to 1200 °C in the presence of carbon reductant, as follows:

(a) The dehydroxylation process with the transformation of goethite (FeOOH) to hematite Fe_2O_3) at 150-320 °C:

$$2\ FeOOH(s) \rightarrow Fe_2O_3(s) + H_2O(g) \tag{4}$$

(b) Volatile matter decomposition at 350-520 °C:

$$\text{Coal (volatile matter)} + O_2(\text{or } H_2O) \rightarrow CO + CO_2 + H_2O + H_2 + CH_4 + \text{other hydrocarbons} + \text{tar} + \text{char} + \text{ash} \quad (5)$$

(c) Reduction of hematite (Fe_2O_3) with the formation of magnetite (Fe_3O_4) at 600-680 °C:

$$3\ Fe_2O_3(s) + C(s)/CO(g) \rightarrow 2\ Fe_3O_4(s) + CO/CO_2(g) \quad (6)$$

(d) Reduction of magnetite (Fe_3O_4) with the formation of wustite (FeO) at 840- 1000 °C:

$$Fe_3O_4(s) + C(s)/CO(g) \rightarrow 3FeO(s) + CO/CO_2(g) \quad (7)$$

(e) Reduction of wustite (FeO) with the formation of metallic iron (Fe_m) at 1020-1140 °C:

$$FeO(s) + C(s)/CO(g) \rightarrow Fe(s) + CO/CO_2(g) \quad (8)$$

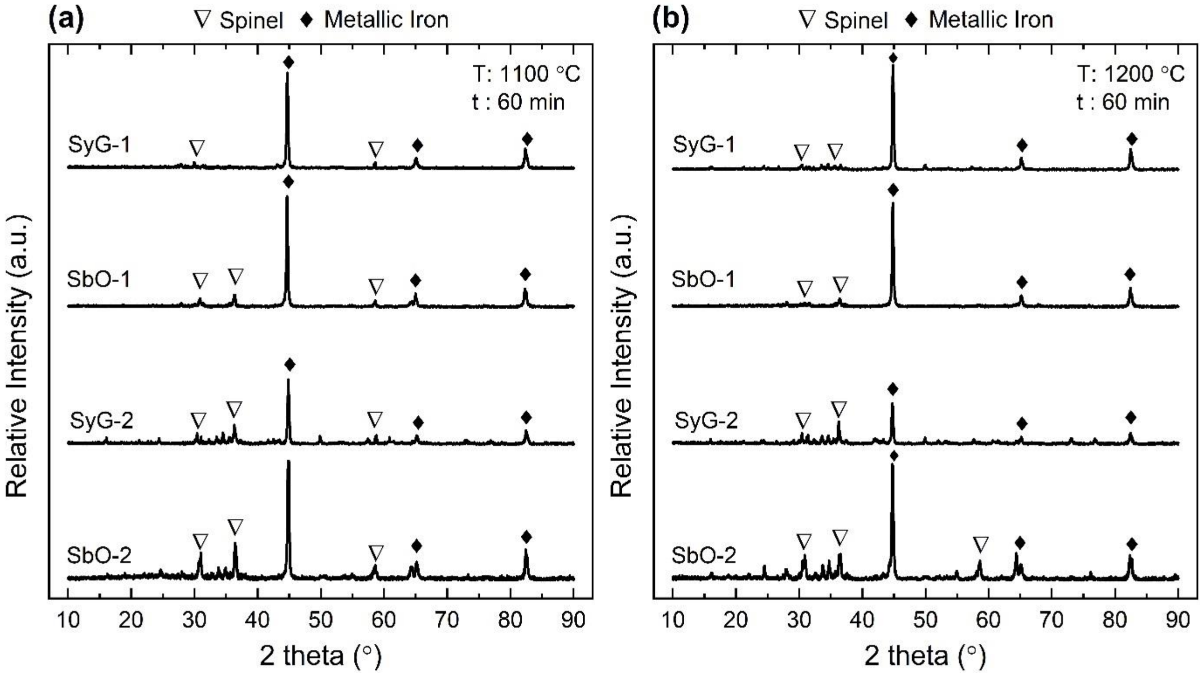

FIGURE 11. XRD analysis results of Sebuku ore (SbO-1 and SbO-2) and synthetic goethite (SyG-1 and SyG-2) samples after reduced for 60 min at: (a) 1100 °C and (b) 1200 °C

CONCLUSION

The carbothermic reduction behavior of low-grade iron ore containing goethite and its comparison with synthetic goethite samples have been investigated. It was found that with the increasing temperature and time of reaction, the volume shrinkage of the Sebuku iron ore and synthetic goethite was greatly enhanced. The maximum volume shrinkage in these samples was observed after reduction at 1200 °C for 60 min, i.e. 63.57±0.57 and 76.51±1.53% for Sebuku ore and synthetic goethite samples, respectively. At this point, the reduction was near to completion. The difference in volume shrinkage is influenced by the loss of oxygen, combined water, and carbon from the system and the presence of impurities in the iron ore (such as Mg, Mn, Al, and Si). Furthermore, the characterization results conducted in this study show the close interrelation between reduction degree, metallization degree, and the volume shrinkage.

ACKNOWLEDGEMENTS

The authors would like to thank the Directorate of Research and Public Engagement, Universitas Indonesia, for this study under PITTA Grant 2018 (2536/UN2.R3.1/HKP.05.00/2018) and PUTI Kolaborasi Internasional 2020 (No. NKB-797/UN2.RST/HKP.05.00/2020).

REFERENCES

Abd Rashid, R.Z., Salleh, H.M., Ani, M.H., Yunus, N.A., Akiyama, T. & Purwanto, H. 2014. Reduction of low grade iron ore pellet using palm kernel shell. *Renewable Energy* 63: 617-623.

Ford, R.G. & Bertsch, P.M. 1999. Distinguishing between surface and bulk dehydrationdehydroxylation reactions in synthetic goethites by highresolution thermogravimetric analysis. *Clays and Clay Minerals* 47(3): 329-337.

Ghose, S.K., Waychunas, G.A., Trainor, T.P. & Eng, P.J. 2010. Hydrated goethite (α-FeOOH) (1 0 0) interface structure: ordered water and surface functional groups. *Geochimica et Cosmochimica Acta* 74(7): 1943-1953.

Halder, S. & Fruehan, R.J. 2008a. Reduction of iron-oxide-carbon composites: part II. Rates of reduction of composite pellets in a rotary hearth furnace simulator. *Metallurgical and Materials Transactions B* 39(6): 796-808.

Halder, S. & Fruehan, R.J. 2008b. Reduction of iron-oxide-carbon composites: Part III. shrinkage of composite pellets during reduction. *Metallurgical and Materials Transactions B* 39(6): 809-817.

Jang, K.O., Nunna, V.R., Hapugoda, S., Nguyen, A.V. & Bruckard, W.J. 2014. Chemical and mineral transformation of a low grade goethite ore by dehydroxylation, reduction roasting and magnetic separation. *Minerals Engineering* 60: 14-22.

Liu, H., Chen, T., Zou, X., Qing, C. & Frost, R.L. 2013. Thermal treatment of natural goethite: Thermal transformation and physical properties. *Thermochimica Acta* 568: 115-121.

McCann, G., Strezov, V., Lucas, J.A., Evans, T. & Strezov, L. 2004. Iron ore characterisation during high temperature thermal processing. *Developments in Chemical Engineering and Mineral Processing* 12(3-4): 369-382.

Merk, R. & Pickles, C.A. 1988. Reduction of ilmenite by carbon monoxide. *Canadian Metallurgical Quarterly* 27(3): 179-185.

Miura, K., Miyabayashi, K., Kawanari, M. & Ashida, R. 2011. Enhancement of reduction rate of iron ore by utilizing low grade iron ore and brown coal derived carbonaceous materials. *ISIJ International* 51(8): 1234-1239.

Ogbezode, J., Ajide, O., Ofi, S. & Oluwole, O. 2021. Determination of the reaction rate controlling resistance of goethite iron ore reduction using CO/CO_2 gases from wood charcoal. *Materials Proceedings* 3(1): 27.

Ponomar, V.P. 2018. Thermomagnetic properties of the goethite transformation during high-temperature treatment. *Minerals Engineering* 127: 143-152.

Prusti, P., Barik, K., Dash, N., Biswal, S.K. & Meikap, B.C. 2021. Effect of limestone and dolomite flux on the quality of pellets using high LOI iron ore. *Powder Technology* 379: 154-164.

Ravisankar, V., Venugopal, R. & Bhat, H. 2019. Investigation on beneficiation of goethite-rich iron ores using reduction roasting followed by magnetic separation. *Mineral Processing and Extractive Metallurgy* 128(3): 175-182.

Sarkar, B.K., Samanta, S., Dey, R. & Das, G.C. 2016. A study on reduction kinetics of titaniferous magnetite ore using lean grade coal. *International Journal of Mineral Processing* 152: 36-45.

Schwertmann, U. 1984. The double dehydroxylation peak of goethite. *Thermochimica Acta* 78(1-3): 39-46.

Setiawan, A., Suratha, R.P., Harjanto, S. & Kusrini, E. 2019. Production of pig iron nugget from low-grade iron ore and pyrolyzed oil-palm-empty-fruit-bunch composites. In *IOP Conference Series: Materials Science and Engineering* 602(1): 012073.

Valix, M. & Cheung, W.H. 2002. Study of phase transformation of laterite ores at high temperature. *Minerals Engineering* 15(8): 607-612.

Wang, G., Wang, J. & Xue, Q. 2018. Kinetics of the volume shrinkage of a magnetite/carbon composite pellet during solid-state carbothermic reduction. *Metals* 8(12): 1050.

Wang, G., Xue, Q. & Wang, J. 2015. Volume shrinkage of ludwigite/coal composite pellet during isothermal and non-isothermal reduction. *Thermochimica Acta* 621: 90-98.

Wang, Q.Y., Wu, Y., Li, Y.H. & Yang, X. 2015. Biomass reduction roasting-magnetic separation of low grade goethite. In *Materials Science Forum*. Trans Tech Publications Ltd. 814: 235-240.

Weissenborn, P.K., Dunn, J.G. & Warren, L.J. 1994. Quantitative thermogravimetric analysis of haematite, goethite and kaolinite in Western Australian iron ores. *Thermochimica Acta* 239: 147-156.

World Steel Association. 2020. *Steel Statistical Yearbook 2019 Concise Version*. World Steel Association.

Yellishetty, M., Ranjith, P.G. & Tharumarajah, A. 2010. Iron ore and steel production trends and material flows in the world: is this really sustainable? *Resources, Conservation and Recycling* 54(12): 1084-1094.

Yu, Y. & Qi, C. 2011. Magnetizing roasting mechanism and effective ore dressing process for oolitic hematite ore. *Journal Wuhan University of Technology, Materials Science Edition* 26(2): 176-181.

[*]Corresponding author; email: sri.harjanto@ui.ac.id